OPTIMAL DESIGN OF KINETIC ENERGY IMPACT ASTEROID ORBIT BASED ON MULTIPLE SPACECRAFT

Fan Wenbao[(1)], Zheng Shigui[(2)] , Meng Qingliang[(1)], KinThong Lee[(1)], and Wang Zhaokui[(1)]

[(1)] *School of Aerospace Engineering, Tsinghua University, fwb20@mails.tsinghua.edu.cn*
[(2)] *Beijing Spacecraft General Design Department, 448035791@qq.com*

ABSTRACT

Asteroid impacts may be the blasting fuse of several extinctions of life on the earth. Preventing severe asteroid meteorite impact catastrophe and improving asteroid defense capabilities are the issues that mankind has always faced. Among all asteroid defense methods, kinetic energy impact technology has the highest maturity. Although the collision velocity in kinetic energy impact method is extremely fast, the impactor may only change the asteroid's velocity by a few millimeters per second because of the wide disparity in mass. The deflection effect of a single spacecraft is finite, and only increasing the impact speed has feeble influence on enhancing asteroid deflection distance. In order to achieve the goal of planetary defense, this paper, taking Apophis as an example, proposes a multi spacecraft kinetic energy impact defense scheme, and studies the ability of multi spacecraft impact scheme consisting of 25 spacecraft to change the distance between Apophis and earth in 2029 and 2036. The paper quickly evaluates the speed increment required for intercepting orbit and the launch window of intercepting spacecraft by using the Lambert method. In addition, Small thrust transfer scheme is adopted for the spacecraft and an optimization method for spacecraft transfer trajectory during interception is proposed in the paper. This paper also proposes an estimation method of momentum enhancement factor β for M-type asteroids based on existing experimental data results. Last but not least, the correctness and optimality of the simulation results in this paper are demonstrated at the same time. From the simulation results, the kinetic energy impact defense method of multiple spacecraft can significantly improve the maximum deflection distance of asteroids when the warning time is short.

Nomenclature

q: Perihelion distance

Q: Aphelion distance

a: Semi-major axis

μ: Gravitational constant

β: Momentum enhancement factor

β_n: The normal components of momentum transfer efficiency

γ_t: The tangential components of momentum transfer efficiency

Δv: Asteroid speed change amount

U, v_{impact}, v_r: Impact velocity between spacecraft and asteroid

v_{ast}: Velocity of an asteroid around the sun in orbit

ω_{ast}: the asteroid's angular velocity

v_r: Relative velocity of spacecraft and asteroid

v_{imp}: The absolute velocity (range) of the spacecraft when it collided with the asteroid

M: target asteroid mass

m: space impactor mass

p_e: A summation of ejecta momentum including fragments from both the impactor and the target

$\hat{n}$: The inward surface normal unit vector

$\hat{t}$: The downrange directed surface tangent unit vector

X, y, z: Denoted as $\{i, j, k\}$, in which k is opposite to v_r, i is a normalization of the cross-product between ω_{ast} (j) and k

X, Y, Z: The coordinate system direction of the heliocentric ecliptic coordinate system

θ_{imp}: Oblique impact angle

θ: Polar angle

ϕ: Azimuthal angle

α: The angle between v_{ast} and v_r

T_{max}: Maximum thrust amplitude

u: Normalized thrust

α_T: Thrust unit direction

I_{sp}: Spacecraft specific impulse

g_0: Ground gravity acceleration

q, a: State variables, $q = ln(m)$, $a = T/m$

v_{ex}: Propellant ejection velocity

$\lambda_r, \lambda_v, \lambda_q$: Covariate variable

e: Euler number

t_0: Departure time

t_f: Arrival time

J_1: Optimization index for fuel optimization problem

Δv_{loc}: The change in asteroid velocity at a specified impact position at a given impact angle

θ_i: Impact angle of the impactor i

$S_{imp\theta_i}$: Effective impact area at angle θ_i

$\overline{\Delta v_{\theta_i}}$: Average speed change at angle θ_i

Δv_{sum}: The total amount of orbital tangential velocity changes caused by all spacecraft impacting asteroids

n: The limited number of spacecrafts

v_{asti}: Absolute velocity of the asteroid at the time of impactor i impact

Acronyms/ Abbreviations

NEOs: Near-Earth Objects

NEAs: Near-Earth Asteroids

NECs: Near-Earth Comets

PHAs: Potentially Hazardous Asteroids

AU: Astronomical Unit

MOID: Minimum orbit intersection distance

DART: Double Asteroid Redirection Test

1. Introduction

Since the 20th century, with the continuous development of human space science and the continuous improvement of space observation capabilities, humans have increasingly focused on the issue of asteroid defense. Scientists believe that asteroid impacts have been the trigger for several mass extinctions on Earth, and an asteroid with a diameter of 5km or larger colliding with Earth can trigger a global mass extinction event. [1,2] In recent years, a series of asteroid hazard events in the solar system have sounded the alarm for humans. In 1994, the observation of the Shoemaker-Levy 9 comet's 21 fragments hitting Jupiter in just over five days was equivalent to the continuous bombing of 500 million atomic bombs over Jupiter's atmosphere in nearly 130 hours, releasing energy equivalent to over 100 trillion tons of TNT explosive. [3] In 2013, the Chelyabinsk event in Russia occurred when an asteroid with a size of less than 18 meters exploded and disintegrated while passing through the atmosphere over Russia, and the resulting debris caused nearly 1,500 injuries and economic losses of over 1 billion rubles. It's not exaggerated to say that asteroid impacts are one of the greatest threats to the entire ecological system on Earth.

By March 15, 2023, a total of 31570 NEOs had been discovered, which are asteroids and comets with perihelion distance q less than 1.3 AU. The vast majority of NEOs are NEAs. Among them, NEAs with a minimum orbital intersection distance (MOID) of within 0.05 AU and an absolute magnitude of H<22 (assuming an albedo of 0.14, corresponding to a diameter of about 140 meters) are defined as PHAs to Earth.[4]
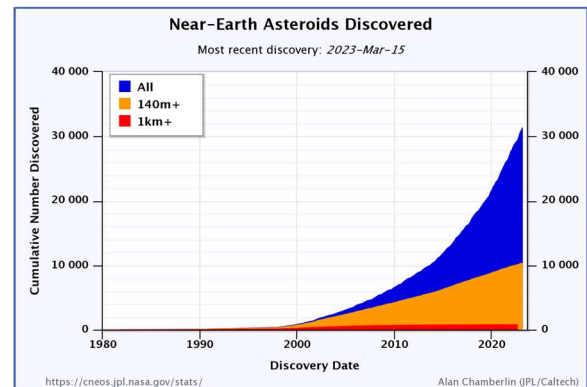

Fig.1. NEAs discovered statistics [5]

In order to defend against PHAs, humans have proposed various NEAs' defense methods. According to the warning time and the size of NEAs, these methods can be roughly divided into three categories: long-term impact deflection, kinetic energy impact, and nuclear explosion strike.[6] Small NEAs with a diameter of less than tens of meters will undergo air explosions during their passage through the Earth's atmosphere, with most of their mass being eroded in the atmosphere, and only a small portion reaching the ground. There is no need to take extraterrestrial defense measures for smaller asteroids. The slow push method is used to change the speed of small near-Earth objects by applying a continuous and stable force to them. It is generally applicable to small near-Earth objects with a defense warning time of several decades and a diameter of less than a few hundred meters. It mainly includes mass drive, gravitational tug, solar light pressure, laser ablation, ion beam traction, and other methods.[7] However, these methods currently have serious limitations in terms of overall performance, cost or technical readiness. The nuclear explosion strike method is to change the orbit of NEOs or destroy them through confrontation or surface explosions. This method is currently an effective method for mitigating the impact of small near-Earth objects with a warning time of less than a few years and a diameter of more than a few hundred meters on the Earth. However, international treaties prohibit nuclear explosion experiments in outer space. The kinetic energy impact method allows small near-Earth objects (NEOs) to obtain a small amount of velocity change through high-speed impact of the impactor, deviating from their original catastrophic orbit. According to current human capabilities to launch the impactor, the kinetic energy impact technology is effective for NEOs with a diameter of less than 1 km. [8]
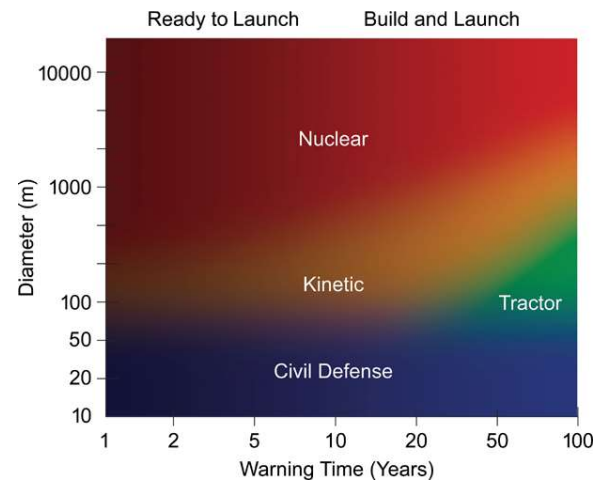

Fig.2. Applicable range of different defense technologies [6]

Among all asteroid defense methods, the kinetic energy impact technology has the highest maturity, which is the only asteroid defense method that has been actually used. The Deep Impact mission conducted by NASA in 2005 facilitated the use of this technology to understand the internal structure and composition of comets, and the Dart mission in 2022 is to demonstrate the technology's effectiveness, which involves deflecting an asteroid (Dimorphs) off its course by colliding with it at approximately 6.2km/s. [9] However, the impact to Dimorphs can only bring a speed change of approximately 0.4 millimeters per second. In future planetary defense missions, such a small speed change may not be sufficient to withstand asteroid threats. Therefore, this paper first studies the impact model based on momentum enhancement factor β and the optimal Kinetic-Impact Geometry method [10] so as to analyze the impact of the ejectors generated by the collision on the amount of velocity change and the effect of planetary deflection. In addition, this paper proposes a multi spacecraft interception trajectory optimization strategy based on the kinetic energy impact method, and takes Apophis as an example to demonstrate the effectiveness of this strategy.

2. Impact Model

In kinetic impact scenarios, the target asteroid gains momentum not only from the incoming impactor but also from the ejecta that escape in the opposite direction of the impact impulse. The combined

momentum is considered to be of a similar magnitude to the directly delivered momentum. Therefore, the momentum enhancement factor β, which is the ratio between total delivered momentum and impactor momentum, is typically greater than 1.

Understanding the asteroid's shape and how the impact location and direction contribute to its velocity change is crucial for designing kinetic-impact missions, especially during the approaching stage. Scheeres et al. [11] discovered non-Gaussian deviations in momentum delivery due to the uncertainty of impact location and β. Feldhacker et al. [12] presented stochastic results on 21 asteroid models by converting the uncertainty in impact location to the probability of hitting a facet. Brack and McMahon [13] examined the effects of momentum transfer deflection on a small body's rotational state and considered the velocity change resulting from different impact locations and directions. Yifei Jiao et al presents a simple and innovative application of Δv hodograph to the optimal geometry design in kinetic deflections of PHAs, as a connection of hypervelocity impact and long-term orbital dynamics.[10] In combination with actual mission conditions, this paper further optimizes the impact model based on previous experience and ground experimental data done by our team.

2.1 momentum enhancement factor β

The concept of β, a measure of momentum transfer efficiency in kinetic impact scenarios, was first proposed by Housen and Holsapple in 2011. Their work included a groundbreaking sputtering scaling law theory, which leveraged point source theory and dimensionless analysis to provide a detailed theoretical description of the mass, velocity, and position distribution of sputtering objects.[14] Building on this foundation, Holsapple further refined the calculation method for β in 2012, focusing specifically on the impact of small celestial bodies. [15] This work helped to shed light on the complex interactions that occur during kinetic impact scenarios, and has proven invaluable for designing and planning future missions in this area.
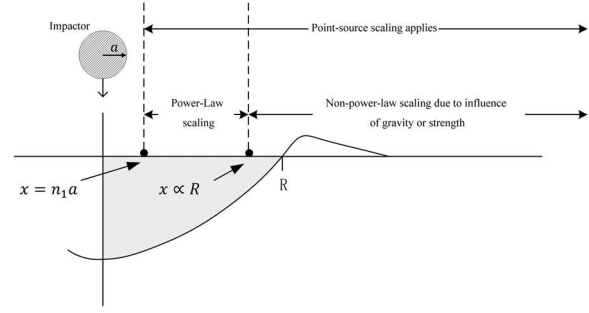

Fig.3. Applicable range of point source theory

β is closely related to the collision velocity and the physical characteristics of the target asteroid. Currently, a large amount of research has been conducted on the β of asteroids of S type and C type [14,15], but less has been done on asteroids of M type, namely, metallic asteroids.
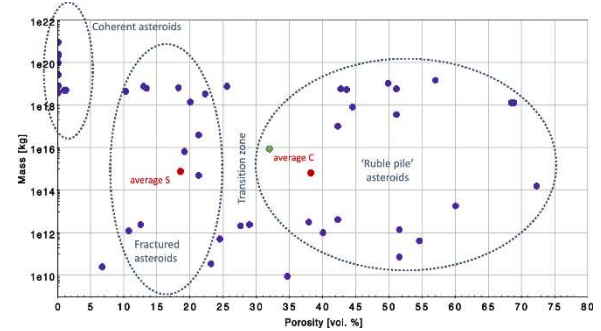

Fig.4. Possible internal structure arrangement of gravitational aggregates, based on their macro-porosity [16]

Our team has estimated β of an M-type asteroid with a diameter of about 100 meters based on ground tests and numerical simulation experiments. The preliminary findings of the momentum enhancement curve for M-type asteroids, as derived from fitting analyses, are presented as follows:

$$\beta = 1 + (5.374 \times 10^{-4})U^{0.638}, initial\ data\ fitting \quad (1)$$
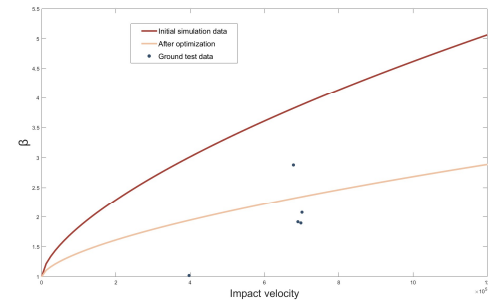$$\beta = 1 + (2.955 \times 10^{-4})U^{0.626}, after\ optimization \quad (2)$$

Fig.5. Relationship between β obtained from simulation test and impact velocity

The algorithm implemented in numerical simulations for hypervelocity collision problems is the material point method (MPM), which combines Lagrange particles with Eulerian background grids. This technique offers numerous advantages in solving coupled solid, fluid, and gas problems, including the capability to accurately describe phase transition phenomena. [17] As such, it has become a popular and effective approach for modeling hypervelocity collisions, allowing for detailed analysis of the dynamics and effects of such events. In terms of material settings, the numerical simulations for hypervelocity collisions involving an aluminum projectile with a density of 2700kg/m3 employ the Simple-Johnson–Cook strength and fracture model [18], combined with the Gruneisen equation of state [19]. The target asteroid is initially modeled as iron ore materials with a density of approximately 7000 kg/m3, for which the Johnson–Cook model is deemed appropriate due to its suitability for high strain rates and high pressures. The use of these models allows for comprehensive analysis of the complex phenomena occurring during hypervelocity collisions, including the behavior of materials under extreme conditions and the potential for damage and fragmentation.[20]
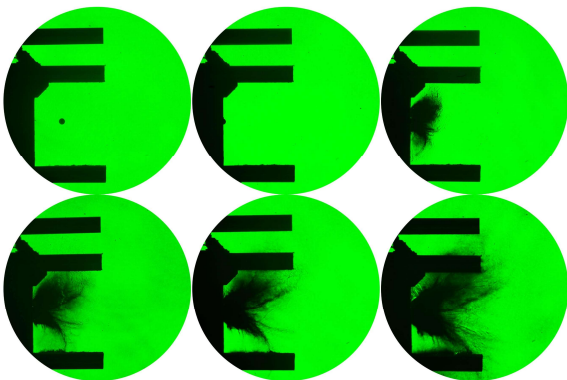

Fig.6. A ground Test Plume Shadows

Before adjustments were made to the modeling, a significant discrepancy existed between ground tests and numerical simulations, largely due to differences in the target materials used for experimental and simulated asteroids. Furthermore, given the constrained number of ground-based tests and limitations in measurement accuracy, it is essential to enhance the testing procedures to obtain a more robust

fitting curve. In an effort to simulate the porosity of an asteroid, ground tests employed molten iron to pour pebbles and create the target material. Once modeling adjustments were optimized, the numerical simulation experiment achieved strong alignment with ground test data, with deviations no greater than 20% when velocities were under 8 km/s. Presently, ground-based experiments and numerical simulation tests are currently ongoing, and it is anticipated that the final results will yield further improvements as additional data is obtained.

2.2 Optimal kinetic-impact Geometry model

The optimal impact geometry model was originally proposed by Jiao Yifei et al., who mainly decomposed the momentum enhancement factor β in the inward planetary surface normal ($\hat{n}\ direction$: β_n) and downrange directed planetary surface tangent ($\hat{t}\ direction$: γ_t) directions in case of oblique impact, as shown in Fig.7, and further derived the Δv hodograph based on the geometric relationship and formula derivation. [10]
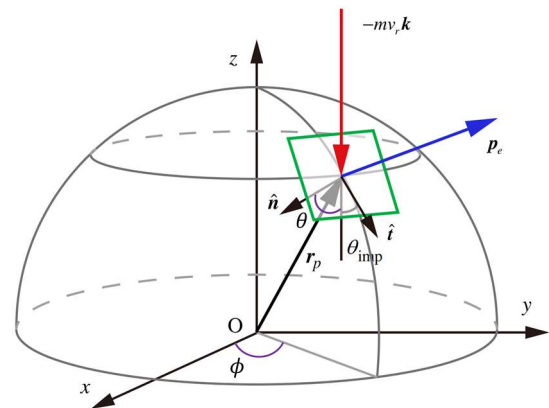

Fig.7. Momentum transfer for a given impact site on an asteroid surface

Firstly, the relationship between Δv and $\beta_n \& \gamma_t$ is derived based on the law of conservation of momentum (ignoring external forces). Through the geometry relationship we can further draw a conclusion that Δv in Eq. (6) is only determined by the inward surface normal $\hat{n}$ at the impact site, for a specific asteroid and impactor. The research of Elbeshausen, D. et al. has given the restriction of θ_{imp} in Eq. (7). An oblique impact with an angle of incidence, denoted as

θ_{imp}, that is less than 30 degrees may result in the projectile ricocheting off the target surface. Additionally, the cratering process in such cases exhibits distinct differences from those of moderate impact angles. [21] In addition, by introducing azimuthal angle ϕ and polar angle θ , Eq. (10) was derived. The specific formula derivation process is as follows:

$$M\Delta v + p_e = m v_r \qquad (3)$$

$$\Delta v = \frac{m}{M}[v_r + (\beta_n - 1)(v_r \cdot \hat{n})\hat{n} + (\gamma_t - 1)(v_r \cdot \hat{t})\hat{t}]$$
$$= \frac{m}{M}[\beta_n(v_r \cdot \hat{n})\hat{n} + \gamma_t(v_r \cdot \hat{t})\hat{t}] \qquad (4)$$

$$\hat{t} = \frac{(k \times \hat{n}) \times \hat{n}}{\| k \times \hat{n} \|} \qquad (5)$$

$$\Delta v = \frac{m v_r}{M}[-\beta_n(k \cdot \hat{n})\hat{n} + \gamma_t(k \times \hat{n}) \times \hat{n}] \qquad (6)$$

$$\theta_{\text{imp}} = \frac{\pi}{2} - \cos^{-1}(-k \cdot \hat{n}) \in \left[\frac{\pi}{6}, \frac{\pi}{2}\right] \qquad (7)$$

$$\hat{n} = -\sin\theta\cos\phi\, i - \sin\theta\sin\phi\, j - \cos\theta\, k \qquad (8)$$

$$\Delta v = \frac{m v_r}{2M}[(\gamma_t - \beta_n)(\sin 2\theta\cos\phi\, i + \sin 2\theta\sin\phi\, j \qquad (9)$$
$$\cos 2\theta\, k) - (\gamma_t + \beta_n)k]$$

$$\left\| \Delta v + (\gamma_t + \beta_n)\frac{m v_r}{2M}k \right\| = \left|(\gamma_t - \beta_n)\frac{m v_r}{2M}\right| \qquad (10)$$

Eq. (10) means that the Δv hodograph can be simplified to a spherical surface when both β_n and γ_t are constant, according to mathematical deduction. The Fig.8 can provide a better understanding of the formation process of the Δv hodograph.
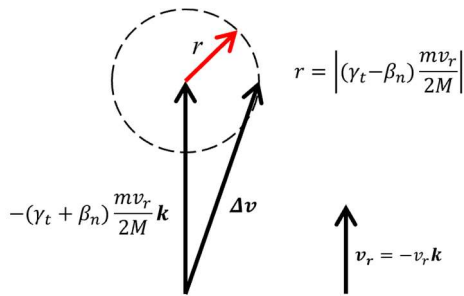

Fig.8. Source of Δv hodograph

Fig.9 presents a near-optimal solution of kinetic impact in this simplified case. As mentioned in Eq. (9), the polar angle of Δv extremity relative to the hodograph center is exactly 2θ, double the polar angle of $\hat{n}$. For an orbital geometry angle of α, the optimal solution suggests a polar angle of the impact normal with $\theta = (1/2)\alpha$. It is worth noting that this conclusion only holds when β_n and γ_t are constants.
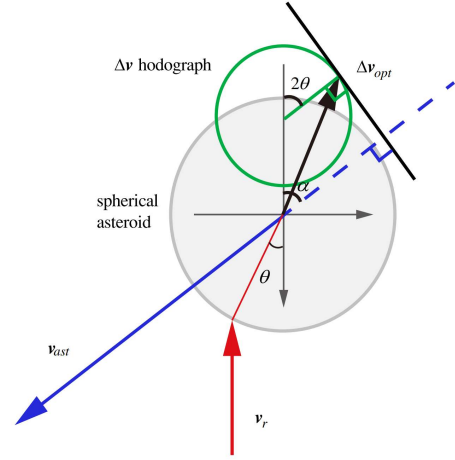

Fig.9. Near-optimal kinetic-impact deflection for a spherical target ($when\ \beta_n\ and\ \gamma_t\ are\ constant$) [10]

The proposed model has the potential to significantly increase deflection efficiency by up to 50% or double it. However, achieving this level of improvement requires precise determination of the impact location in the case of oblique impacts. When the oblique impact angle is held constant, larger deviations in the impact location can lead to negative gains in deflection effectiveness, as illustrated in Fig.10. The ratio on the right side of the Fig.10. shows the ratio between Δv generated by oblique impact and Δv generated by frontal impact. When the ratio exceeds 1, it indicates that the deflection effect is enhanced, and vice versa, the deflection effect is reduced.
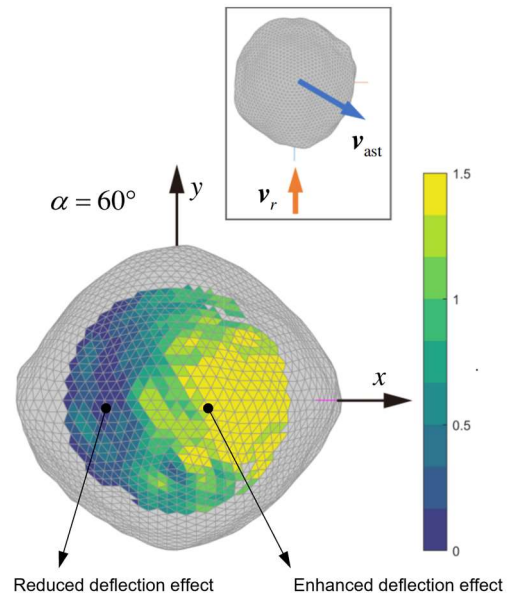
Fig.10. Distribution of Δv ratio for various impact locations when $\alpha = 60^{\circ}$ [10]

In practical defense scenarios, the magnitude of the α is determined by the orbital geometry [22], and the coefficients a and b in this model are obtained by semi-analytical fitting of the similarity rate model, which may deviate from the actual scenario. Furthermore, the gravitational attraction between the sun and the asteroid can affect the deflection caused by oblique impacts. Hence, it is imperative to design appropriate deflection trajectories.

3. Orbit Design for Multiple Spacecraft Interception

To facilitate the practical optimization of orbit design, this study initially formulated a high-precision orbit model for Apophis, which considers various perturbations, including solar pressure, gravitational perturbation of the eight planets, etc. [23] The discrepancy between this model and NASA's ephemeris from 2010 to 2040 is less than 1%, as depicted in Fig.11, indicating a high level of accuracy. Furthermore, utilizing this orbit model, a plot indicating the variation of Apophis's distance from the Earth during the period from 2010 to 2040 was also constructed, as shown in Fig.12.
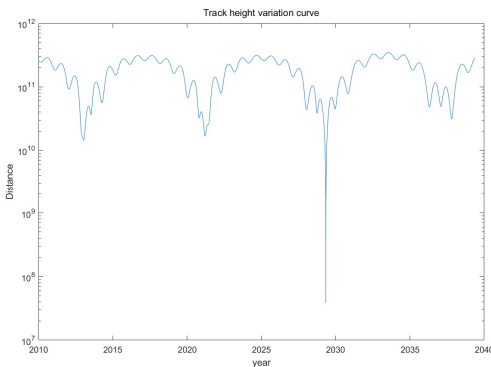

Fig.11. Distance variation curve between Apophis and earth
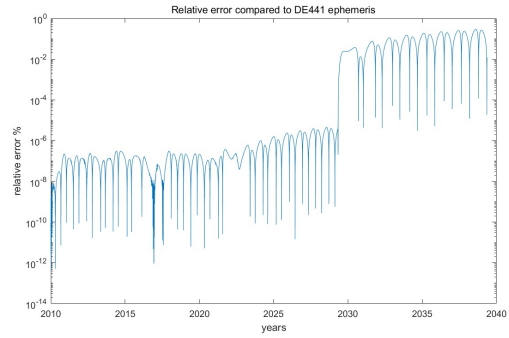

Fig.12. Relative error of position vector Apophis

To determine parameters such as departure time, arrival time, and required velocity increment for the transfer orbit of the impactor, a total velocity increment diagram for transfer orbit times up to 2 years has been presented in Fig.13. This diagram is specifically designed for the exploration of Apophis asteroid and offers a detection departure time selection range spanning from January 1, 2023 to January 1, 2028. In Fig.13, the horizontal axis corresponds to the elapsed time relative to January 1, 2023, while the vertical axis represents the flight duration of the impactor. The color mapping scheme indicates the required velocity increment (km/s) during the flight process, as calculated using Lambert's method. Darker colors correspond to lower velocity increments, resulting in a larger remaining mass and higher momentum at the same terminal velocity. The diagram shows multiple launch windows for intercepting the Apophis asteroid, and based on the results, the launch window from April 5 to April 15, 2028, which requires a speed increment of less than 5 km/s during the flight process, appears to be the most favorable option.
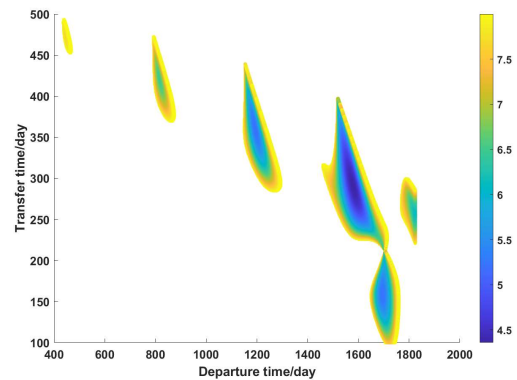

Fig.13. Departure time and incremental changes in spacecraft required speed

Given the launch time, transfer time, and the time of collision or closest approach between the asteroid and Earth, the velocity change Δv required by the spacecraft to deflect the asteroid can be calculated using the impact model, which yields the absolute velocity range (v_{imp}) at which the spacecraft will intercept the asteroid. When determining the transfer time and terminal velocity of a designated spacecraft, minimizing fuel consumption leads to a higher residual mass, greater momentum, and improved deflection effect. Therefore, the orbit optimization problem with maximum momentum at collision is thus reduced to an optimization problem of minimizing the spacecraft's fuel consumption subject to special constraints and fixed time intervals. The index for this optimization problem can be expressed as acceleration:

$$minJ_1 = \frac{1}{v_{ex}}\int_{t_0}^{t_f} T_{max}udt = \frac{1}{v_{ex}}\int_{t_0}^{t_f} ae^q dt \qquad (11)$$

The definitions of each symbol can be found in the nomenclature at the beginning of this paper. Further introduce the Covariate variable $[\lambda_r, \lambda_v, \lambda_q]$ to construct the Hamiltonian function as:

$$H_1 = \lambda_r \cdot \boldsymbol{v} + \lambda_v \cdot \left(-\frac{\mu}{r^3}\boldsymbol{r} + a\boldsymbol{\alpha}\right) + \lambda_q\left(-\frac{a}{v_{ex}}\right) + \frac{ae^q}{v_{ex}} \quad (12)$$

According to the principle of Pontryagin's Minimum Principle (PMP), optimal control means that the Hamiltonian function takes the minimum value. [24] The opposite direction of the thrust direction satisfying the speed co-state can be obtained.

$$\alpha_T = -\frac{\lambda_v}{\|\lambda_v\|} \qquad (13)$$

The optimal acceleration is:

$$\begin{cases} a = \frac{T_{max}}{e^q}, s < 0 \\ a = 0, s > 0 \\ 0 < a < \frac{T_{max}}{e^q}, s = 0 \end{cases} \qquad (14)$$

Where the switch function is:

$$s = \frac{\left(e^q - \lambda_q\right)}{v_{ex}} - \|\lambda_v\| \qquad (15)$$

The transversal condition is:

$$\lambda_q\left(t_f\right) = 0 \qquad (16)$$

To sum up, the optimization problem has a total of 7 quantities to be demanded:

$$\boldsymbol{z} = \{\lambda_r(t_0), \lambda_v(t_0), \lambda_q(t_0)\} \qquad (17)$$

Need to satisfy 7 shooting equations:

$$\Phi_1(\lambda^*) = \{\boldsymbol{r}(t_f) - \boldsymbol{r}_f, \boldsymbol{v}(t_f) - \boldsymbol{v}_f - \boldsymbol{v}_r, \lambda_q(t_f)\} = \boldsymbol{0} \ (18)$$

Fig.14 and Fig.15 shows the transfer orbit where May 5, 2028 is selected as the deflection time based on the above optimization method from a three-dimensional perspective and a two-dimensional perspective. The constraint condition is that a single spacecraft can bring a orbital tangential velocity change of 0.3mm/s to the asteroid when it hits. It is noteworthy that this example serves only to demonstrate the need for a multi-spacecraft interception strategy, and is not intended to replicate the significant orbital deviation that would be required in an actual defense mission.[25]
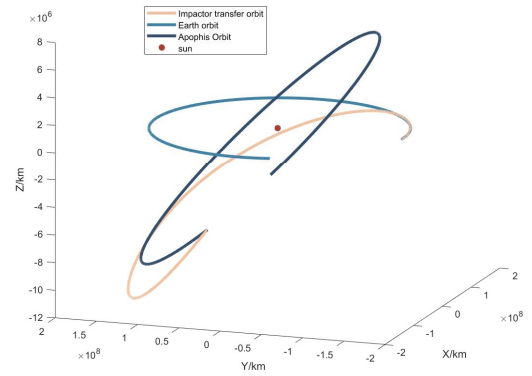

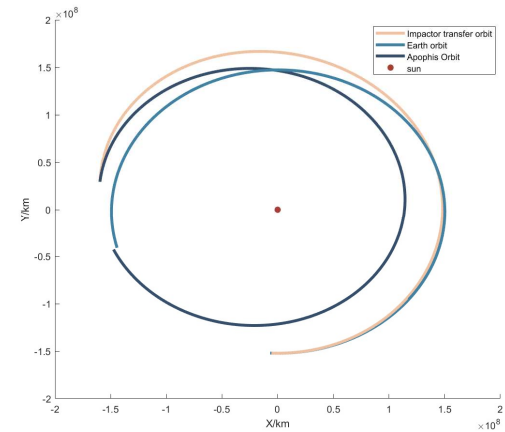Fig.14. Three-dimensional diagram of interception and transfer trajectory of Apophis

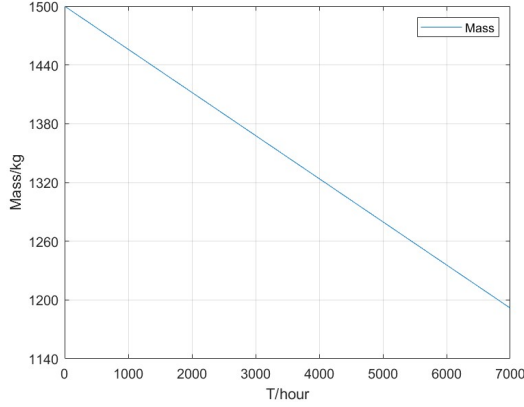Fig.15. Two-dimensional diagram of interception and transfer trajectory of Apophis

Fig.16. Apophis Intercept Transfer Orbit Mass
Variation Chart

Fig.18. Offset distance increase on May 5, 2036
under single spacecraft interception

As can be seen from Fig.16, the spacecraft has been subjected to small thrust acceleration during transfer orbit flight. After the interception by a single spacecraft, the distance between Apophis and Earth will increase in April 10, 2029, and the impact of the launch date disturbance (May 5, 2028~ May 15, 2028) can be observed in Fig.17. (the unit of distance in this figure is "m") In the figure, each point denotes the absolute position of Apophis in the heliocentric ecliptic coordinate system for a distinct launch date. The color of the point reflects the disparity between the distances of Earth from Apophis before and after the offset. A brighter color corresponds to a larger distance difference. The point with the greatest distance difference is associated with the launch date of May 5, 2028, which is 2236m. Fig.18 shows the deflection distance enhancement on May 5, 2036.
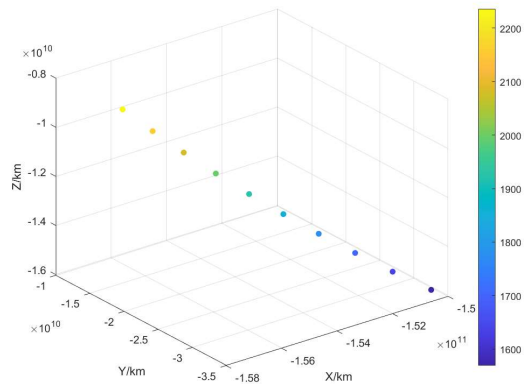

Fig.17. Offset distance increase on April 10, 2029
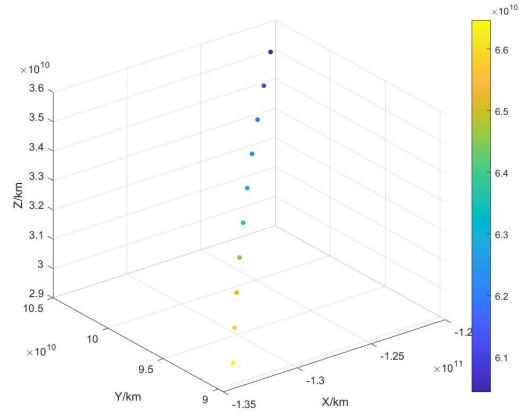under single spacecraft interception

As can be seen from the above results, it can be inferred that the deflection effect of a single spacecraft in a particular planetary defense mission could be considerably weak when the warning time is short. From the standpoint of orbit optimization, the deflection effect of a single spacecraft during the defense could be enhanced by altering the constraint conditions, such as increasing the speed change caused by spacecraft impact on the asteroid, elevating the absolute speed of spacecraft impact, and altering the impact angle. However, the imposition of high constraints may render the optimization equation unsolvable, and the parameters in the equation are restricted by the actual mission requirements and current technological capabilities. Thus, the development of multiple spacecraft optimization strategies is crucial. The following provides the deflection situation of multiple spacecrafts interception. The impact process can be simplified as multiple spacecrafts continuously colliding with Apophis at different angles within a short time interval. The average velocity change under different impact angles can be calculated based on the optimal impact geometry model introduced in the previous section, and the specific formula is as follows:

$$\overline{\Delta v_{\theta_i}} = \iint\limits_{S_{imp\theta_i}} \Delta v_{loc} ds \qquad (19)$$

The total velocity change that the spacecraft bring to Apophis can be expressed as:

$$\Delta v_{sum} = \sum_{i=1}^{n} \left| \frac{\overline{\Delta v_{\theta_i}} \cdot v_{asti}}{\|v_{asti}\|} \right| \qquad (20)$$

Fig.19 and Fig.20 respectively represent the increase in deflection distance on April 10, 2029, and May 5, 2036, under the interception of 25 spacecraft.
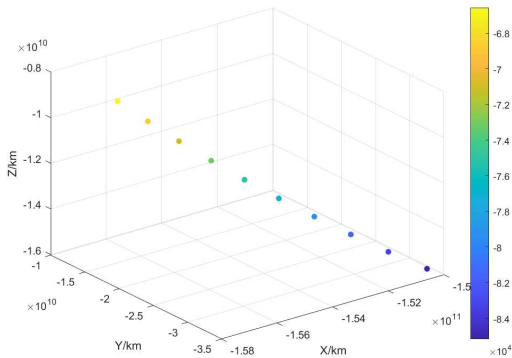

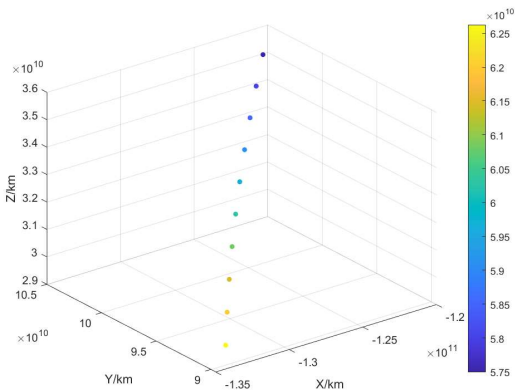Fig.19. Offset distance increase on April 10, 2029 under multiple spacecrafts interception

Fig.20. Offset distance increase on May 5, 2036 under multiple spacecrafts interception

The results of Fig.19 show that the multi spacecraft interception strategy can greatly improve the asteroid deflection effect when the warning time is short. Under the impact of 25 spacecraft, the orbital offset increased by about 31 times in April 2029.In the case of short warning time and large target asteroid size, implementing the multi spacecraft interception strategy can more effectively protect the Earth's homeland.

4. Conclusions

This paper exemplifies the requirement for deploying multiple spacecraft interception strategies in real planetary defense missions through the deflection of Apophis. It proposes an optimization technique for the spacecraft's transfer trajectory during interception and presents an approach to estimate the momentum enhancement factors of metallic asteroids using existing ground experiment and simulation test data. The advantages and limitations of the optimal kinetic impact geometry model are comprehensively and systematically analyzed. The above are only some of the research results of our team. The standardization of interception orbit optimization indicators and the impact of spacecraft launch time series on the final deflection results in multiple spacecraft defense strategies will be released after further improvement.

References

[1] RUMPF C M, MATHIAs D L, WHEELER L F, et al. Deflection driven evolution of asteroid impact risk under large uncertainties[J]. Acta Astronautica, 2020, 176: 276 -286

[2] OSINSKI G R, GRIEVE R, FERIERE L, et al. Impact Earth: A review of the terrestrial impact record[J]. Earth science Reviews, 2022, 232: 104112.

[3] Fu Chengqi. Summary of the Comet Wood Collision Event [J]. Science,1994,46(05):60-61

[4] The International Astronomical Union Minor Planet Center [Z/OL]. [2023/03/17]. https://minorplanetcenter.net

[5] Center for Near Earth Object Studies Discovery Statistics Cumulative Totals[Z/OL]. [2023/03/17]. https://cneos.jpl.nasa.gov/stats/totals.html

[6] Perna, D., Barucci, M.A. & Fulchignoni, M. The near-Earth objects and their potential threat to our planet. Astron Astrophys Rev 21, 65 (2013). https://doi.org/10.1007/s00159-013-0065-4

[7] 范文宝,杜菲,王兆魁. 金属质小行星在轨处置技术综述[C]//.第三届中国空天安全会议论文集.,2021:261-273. DOI:10.26914/c.cnkihy.2021.024642
Fan Wenbao, Du Fei, Wang Zhaokui Summary of On-orbit Disposal Technologies for Metallic Asteroids [C]//. Proceedings of the Third China Aerospace Safety Conference, 2021:261-273. DOI:10.26914/c.cnkihy.2021.024642

[8] 龚自正,李明,陈川,等. 小行星监测预警、安全防御和资源利用前沿科学问题及关键技术 [J] .科学通报，2020，65 (5) : 346 -372 .
Gong Zizheng, Li Ming, Chen Chuan, et al Frontier scientific issues and key technologies in asteroid monitoring, early warning, security defense, and resource utilization [J]. Science Bulletin, 2020, 65 (5):

346-372.

[9] Double Asteroid Redirection Test [Z/OL]. [2023/03/17]. https://dart.jhuapl.edu.

[10] Yifei Jiao, Bin Cheng, and Hexi Baoyin. Optimal Kinetic-Impact Geometry for Asteroid Deflection Exploiting Delta-V Hodograph. Journal of Guidance, Control, and Dynamics 2023 46:2, 382-389.

[11] Scheeres, D. J., McMahon, J. W., Jones, B. A., and Doostan, A., "Variation of Delivered Impulse as a Function of Asteroid Shape," 2015 IEEE Aerospace Conference, Inst. of Electrical and Electronics Engineers, New York, 2015, pp. 1–7.

[12] Feldhacker, J. D., Syal, M. B., Jones, B. A., Doostan, A., McMahon, J., and Scheeres, D. J., "Shape Dependence of the Kinetic Deflection of Asteroids," Journal of Guidance, Control, and Dynamics, Vol. 40, No. 10, 2017, pp. 2417–2431

[13] Brack, D. N., and McMahon, J. W., "Effects of Momentum Transfer Deflection Efforts on Small-Body Rotational State," Journal of Guidance, Control, and Dynamics, Vol. 43, No. 11, 2020, pp. 2013–2030.

[14] Housen, K. R., and Holsapple, K. A., "Ejecta from Impact Craters," Icarus, Vol. 211, No. 1, 2011, pp. 856–875.

[15] Holsapple, K. A., and Housen, K. R., "Momentum Transfer in Asteroid Impacts. I. Theory and Scaling," Icarus, Vol. 221, No. 2, 2012, pp. 875–887.

[16] Hestroffer, Daniel, et al. "Small solar system bodies as granular media." The Astronomy and Astrophysics Review 27 (2019): 1-64.

[17] 廉艳平,张帆,刘岩,张雄.物质点法的理论和应用[J].力学进展,2013,43(02):237-264.

Lian Yanping, Zhang Fan, Liu Yan, Zhang Xiong. The theory and application of the material point method [J]. Progress in Mechanics, 2013,43 (02): 237-264

[18] Johnson, Gordon R., and Tim J. Holmquist. "Evaluation of cylinder‐impact test data for constitutive model constants." Journal of Applied Physics 64.8 (1988): 3901-3910.

[19] Meyers, Marc A. Dynamic behavior of materials. John wiley & sons, 1994.

[20] Johnson, Gordon R., and William H. Cook. "Fracture characteristics of three metals subjected to various strains, strain rates, temperatures and pressures." Engineering fracture mechanics 21.1 (1985): 31-48.

[21] Elbeshausen, Dirk, Kai Wünnemann, and Gareth S. Collins. "Scaling of oblique impacts in frictional targets: Implications for crater size and formation mechanisms." Icarus 204.2 (2009): 716-731.

[22] Yamaguchi, Kohei, and Hiroshi Yamakawa. "Visualization of kinetic-impact effectiveness for asteroid deflection using impact-geometry maps." Journal of Spacecraft and Rockets 55.5 (2018): 1181-1197.

[23] Giorgini, Jon D. "Status of the JPL horizons ephemeris system." IAU General Assembly 29 (2015): 2256293.

[24] 袁建平，李俊峰，和兴锁. 航天器相对运动轨道动力学[M]. 中国宇航出版社, 2013.

Yuan Jianping, Li Junfeng, He Xingsuo. Spacecraft Relative Motion Orbital Dynamics[M]. China Aerospace Press, 2013.

[25] 李泰博.小行星资源勘探与利用任务的轨迹优化与智能控制[D]. 国防科技大学，2020

Li Taibo. Trajectory optimization and intelligent control of asteroid resource exploration and utilization missions [D] National University of Defense Technology, 2020.